The Functional Role of Binuclear Metal Center in D-aminoacylase One-Metal Activation and Second-Metalattenuation

Our structural comparison of the TIM barrel metal-dependent hydrolase(-like) superfamily suggests a classification of their divergent active sites into four types: αβ-binuclear, α-mononuclear, β-mononuclear and metal-independent subsets. The D-aminoacylase from A. faecalis DA1 belongs to the β-mononuclear subset due to the fact that the catalytically essential Zn^{2+} is tightly bound at the β site with coordination by Cys^{96}, His^{220}, and His^{250}, even though it possesses a binuclear active site with a weak α binding site. Additional Zn^{2+}, Cd^{2+} and Cu^{2+}, but not Ni^{2+}, Co^{2+}, Mg^{2+}, Mn^{2+} and Ca^{2+}, can inhibit enzyme activity. Crystal structures of these metal derivatives show that Zn^{2+} and Cd^{2+} bind at the α_1 subsite ligated by His^{67}, His^{69} and Asp^{366}, while Cu^{2+} at the α_2 subsite is chelated by His^{67}, His^{69} and Cys^{96}. Unexpectedly, the crystal structure of the inactive H220A mutant displays that the endogenous Zn^{2+} shifts to the α_3 subsite coordinated by His^{67}, His^{69}, Cys^{96} and Asp^{366}, revealing that elimination of the β site changes the coordination geometry of the α ion with an enhanced affinity. Kinetic studies of the metal ligand mutants such as C96D indicate the uniqueness of the unusual bridging cysteine and its involvement in catalysis. Therefore, the two metal-binding sites in the D-aminoacylase are interactive with partially mutual exclusion, thus resulting in widely different affinities for the activation/attenuation mechanism, in which the enzyme is activated by the metal ion at the β site, but inhibited by the subsequent binding of the second ion at the α site.

D-aminoacylases (EC 3.5.1.81) is an attractive candidate for commercial production of D-amino acids through its catalysis of the deacetylation of N-acetyl-D-amino acids. Since D-amino acids are intermediates in the preparation of antibiotics, pesticides and bioactive peptides, D-aminoacylase has commercial importance for the optical resolution of N-acetyl-DL-amino acids. The crystal structure of the 483-residue D-aminoacylase from Alcaligenes faecalis DA1 revealed that the enzyme comprises of a small β barrel and a catalytic TIM barrel with a 63-residue insertion. The structural similarity and the conserved metal ligands of four histidines and one aspartate suggest that D-aminoacylase belongs to the TIM barrel metal-dependent hydrolase superfamily. This superfamily includes a variety of enzymes with highly diverse substrates and has been coined an "evolutionary treasure".

To date, crystal structures of fourteen members in the superfamily have been determined. As more structures are solved, more divergences in the metal centers and in the β-strand packing of the TIM barrel are observed (Fig. 1A). Based on the binding site(s) of the catalytically essential metal ion(s), we classify these members into four types: αβ-binuclear (αβ), α-mononuclear (α), β-mononuclear (β) and metal-independent subsets. Phosphotriesterase (homology protein), urease, dihydroorotase, renal dipeptidase, isoaspartyl didpeptidase, and dihydropyrimidinase comprise the αβ subset. Murine adenosine deaminase and *E. coli* cytosine deaminase belong to the α subset. D-aminoacylase belongs to the β subset due to the essential Zn^{2+} binding tightly at the β site, even though it possesses a weak α binding site. In contrast, the activity assay and the crystal structure of uronate isomerase show that this enzyme does not display any specific metal requirement and thus belongs to the metal-independent subset.

The functional requirement for the different metal centers is still unclear. Interestingly, *B. subtilis* *N*-acetylglucosamine-6-phosphate deacetylase (NAGA) contains two iron ions and thus belong to the αβ subset, whereas the *T. maritima* enzyme has only one iron bound at the β site and may belong to the β subset. Structural comparison demonstrates that both αβ and β subsets share similar binuclear active sites (Fig. 1B). The crystal structure of the inactive *K. aerogenes* urease variant (H134A) suggests that the proper coordination for the two catalytically essential metal ions in the αβ subset is mutually cooperative. Therefore, we would like to address the function of the binuclear center in D-aminoacylase, the best studied β member.

The naturally isolated D-aminoacylase with

Fig. 1A

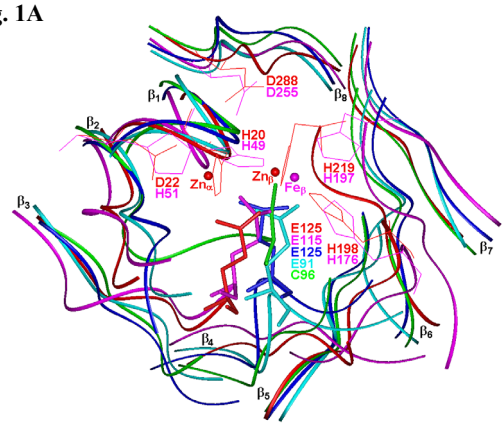

Fig. 1B

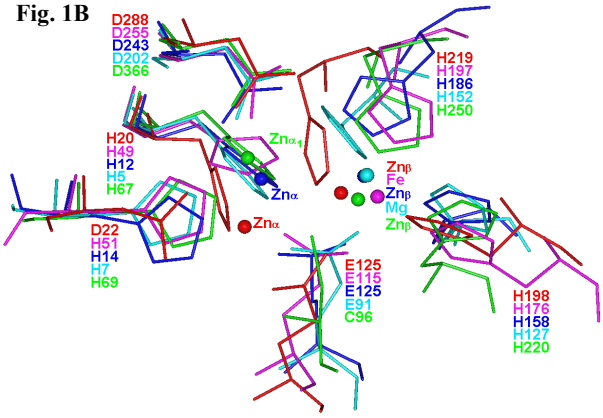

Fig. 1: *Comparison of human renal dipeptidase (red), E. coli phosphotriesterase homology protein (blue), D-aminoacylase (green), T. maritima NAGA (magenta) and T. maritima TatD (cyan), with a close view of the divergent β-strand packing of the TIM barrel (A) and the binuclear metal centers (B). The residue numbering is labeled in the same color for each protein. The α site is constituted by the first two conserved histidines from a common HXH motif at the β1 strand, a bridging ligand, and/or the conserved aspartate at the β8 strand, where the β site is coordinated by the last two conserved histidines at the β5 and β6 strands and the bridging ligand. Most bridging residues are located at the β4 strand, except for the glutamates in human renal dipeptidase and NAGAs at the β3 strand, and the cysteine in D-aminoacylase at the β2 strand. The shift in the sequence position causes larger structural differences.*

out any added metal ion exhibits significant activity. Addition of extrinsic zinc ions is able to strongly inhibit enzyme activity. Zn^{2+} proved to be the most potent inhibitor followed by Cd^{2+} and Cu^{2+}. Our kinetic studies demonstrate that exogenous Zn^{2+} and Cd^{2+} ions attenuate activity by slowing catalysis at the level of the rate-limiting step (a decrease in k_{cat}), characteristic of noncompetitive inhibition. However, Mg^{2+}, Mn^{2+}, Co^{2+}, Ni^{2+} and Ca^{2+} do not inhibit the enzyme activity. Interestingly, addition of Zn^{2+} into the C96D mutant but not the C96A, C96S, H220A and D366A mutants could restore some enzyme activity.

The different metal derivatives were prepared by soaking crystals of the wild-type and mutant enzymes in a metal solution. Difference Fourier maps of various metal derivative structures were examined (Fig. 2). For the Zn^{2+} ion derivative, two strong electron density peaks, one at the natural β site and the other at the α site, were assigned as zinc based on the zinc anomalous data. The zinc ion at the β site is coordinated by Cys^{96}, His^{220} and His^{250} as it is in the native enzyme, while the zinc ion at the α site is tetrahedrally ligated by His^{67}, His^{69}, Asp^{366} and ACT1, an acetate molecule from the crystallization solution. For the Cd^{2+} derivative, the difference Fourier maps also show a large peak at the α site, suggesting that Cd^{2+} ion binds at the same position as the Zn^{2+} ion, henceforth called the α_1 subsite. In contrast, Cu^{2+} is ligated by His^{67}, His^{69}, Cys^{96} and ACT1 at the α_2 subsite. However,Mn^{2+}, Co^{2+}, Ni^{2+} and Ca^{2+} did not bind to the enzyme.

Unexpectedly, the difference electron density maps showed that in the H220A mutant the endogenous zinc ion no longer binds at the β site, instead it is tetrahedrally coordinated by His^{67}, His^{69}, Cys^{96} and Asp^{366} at the α_3 subsite (Fig. 3). The α_3 subsite is located almost midway between the α_1 and α_2 sites. The much stronger electron density peak and lower B-factor of the zinc ion in the H220A mutant than the proposed zinc ion at the α_1 subsite in the native enzyme show that elimination of the β ion enhances the binding affinity of the α ion.

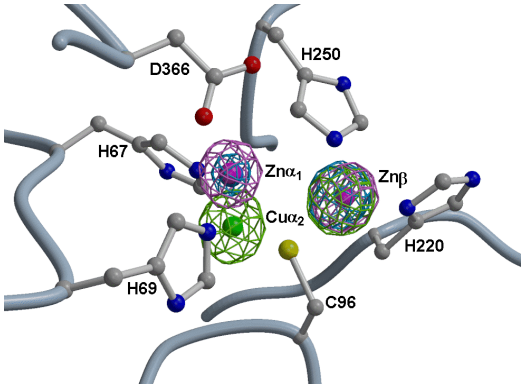

Fig. 2: *The F_o – F_c electron density maps of the native enzyme in complex with 100 mM $ZnCl_2$ contoured at 15σ level and shown in* magenta, *with 50 mM $CdCl_2$ contoured at 15σ level and shown in* cyan, *and with 100 mM $CuCl_2$ contoured at 18σ level and shown in* green. *The metal ligands are shown as a* ball-and-stick *representation, with the Zn^{2+} and Cu^{2+} ions as* magenta *and* green *spheres. Zn^{2+} and Cd^{2+} bind at the α_1 subsite, where Cu^{2+} binds at the α_2 subsite.*

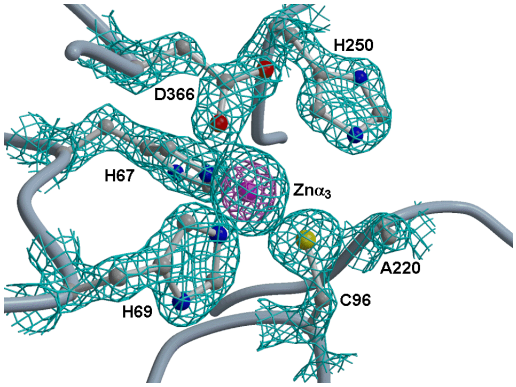

Fig. 3: The $2F_o - F_c$ electron density maps of the H220A mutant contoured at 2.5σ level and shown in cyan, and the difference map for the zinc ion contoured at 15σ level and shown in magenta. The endogenous zinc ion binds at the α_3 subsite instead of the β site in this mutant.

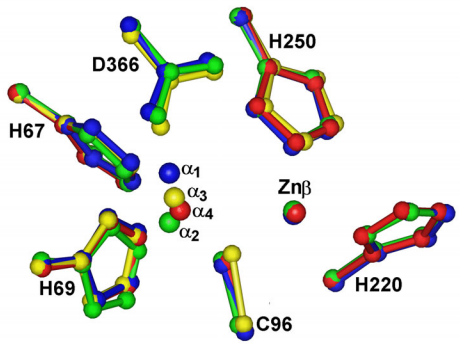

Fig. 4: Superposition of the native enzyme with 100 mM $ZnCl_2$ in blue, the native enzyme with 100 $CuCl_2$ in green, the H220A mutant in yellow, and the D366A mutant with 100 mM $ZnCl_2$ in red. The different metal coordination is carried out by small shifts in the side chains of ligands and small movements of the metal ions.

This enhancement suggests that the α and β sites are interactive with partially mutual exclusion. Cysteine residues have never been found to serve as bridging ligands in the cocatalytic zinc-binding sites. In the native enzyme, Cys^{96} commits most of its charge to interact with the β ion, and thus could not interact with the α ion strongly, resulting in different metal-binding affinities. Once the β site is destroyed, Cys^{96} could contribute its charge to interact with the α ion and thus enhance metal affinity. This unusual bridging Cys^{96} has been shown to contribute the most toward the interactions with the metal ions among the ligands, because the C96A mutant shows very little zinc-binding ability, 0.2 g · atom per mole of enzyme. The less active C96D mutant also demonstrates the uniqueness of this cysteine residue.

In D366A mutant, additional Cu^{2+} binds at the α_2 subsite, the same as in the wild-type protein, while Zn^{2+} binds weakly at another α site (α_4) surrounded by His^{67}, His^{69}, Cys^{96} and ACT1 (Fig. 4). A comparison of the crystal structures presented here reveals that the spatial locations of all protein residues are virtually identical, suggesting that the His^{220} mutant, the Asp^{366} mutant and the metal binding to the enzyme do not significantly alter the three-dimensional structure (Fig. 4). The differences in metal coordination are achieved by small movements of the metal ions and small shifts in the side chains of ligands to accommodate the metal binding. These results seem to be in agreement with the entatic state theory proposed by Williams, in which the metal site in a metalloprotein is configured by the protein matrix. The contrast between virtually identical β sites and conformationally variable α sites with a looser arrangement of ligands, is consistent with their different affinities.

Our studies presented here suggest that the binuclear metal center in D-amioacylases is responsible for a metal activation/attenuation mechanism. The enzyme is activated by the Zn^{2+} ion tightly bound at the β site, but inhibited by the subsequent binding of a second metal ion at the α site. To achieve this mechanism, an unusual bridging cysteine (Cys^{96}) is inserted to generate mutually exclusive metal-binding sites, which result in different metal-binding affinities. The binding at the high affinity β site leads to a weakened binding at the α site, whereas a lack of the β ion enhances the α ion binding. To the best of our knowledge after a structural and sequence search, D-aminoacylase is the only member of the TIM barrel metal-dependent hydrolase superfamily that uses a cysteine as a metal bridging ligand. Mutation of Cys^{96} into alanine, serine and threnine but not aspartate causes an almost complete loss of the metal-binding ability. The purified C96D mutant contains a similar zinc content as measured by atomic absorption, as the native enzyme. However, this mutant results in 10^4-fold decrease in the enzyme activity. Unexpectedly, addition of some zinc ions restores the enzyme activity by 100 fold with an effect on k_{cat} but not K_m, indicating involvement of this cysteine residue in catalysis. Therefore, the particular bridging cysteine residue serves as a control switch for regulation of catalytic activity. Since zinc is the second-most abundant transition metal in living organisms after iron, it is quite possible that inhibitory zinc ions may be involved in important physiological functions and this should not be neglected.

BEAMLINES
17B W20 X-ray Scattering beamline
SP12B Biostructure and Materials Research beamline
41XU SPring-8 beamline

EXPERIMENTAL STATION
Protein Crystallography end station

AUTHORS
S.-H. Liaw
Structural Biology Program, Faculty of Life Science, National Yang-Ming University, Taipei, Taiwan

PUBLICATIONS
· W. L. Lai, L. Y. Chou, C. Y. Ting, R. Kirby, Y. C. Tsai, A. H. J. Wang, and S. H. Liaw, J. Biol. Chem. **279**, 13962 (2004).
· S. H. Liaw, S. J. Chen, T. P. Ko, C. S. Hsu, C. J. Chen, A.H. J. Wang, and Y. C. Tsai, J. Biol. Chem. **278**, 4957 (2003).
· C. S. Hsu, W. L Lai, W. W. Chang, S. H. Liaw, and Y. C. Tsai, Protein Sci. **11**, 2545 (2002).
· C. S. Hsu, S. J. Chen, Y. C. Tsai, T. W. Lin, S. H. Liaw, and A.H. J Wang, Acta Cryst. **D 55**, 1482 (2002).

CONTACT E-MAIL
shliaw@ym.edu.tw